

# MS-TVNet: A Long-Term Time Series Prediction Method Based on Multi-Scale Dynamic Convolution

Chenghan Li<sup>\*\*</sup>, Mingchen Li<sup>†\*</sup>, Yipu Liao<sup>‡</sup>, Ruisheng Diao<sup>§</sup>

<sup>\*</sup>Shenzhen International Graduate School, Tsinghua University, Shenzhen, China

<sup>†</sup>The Hong Kong University of Science and Technology (Guangzhou)

<sup>‡</sup>ECE Department, University of Michigan (Ann Arbor), Ann Arbor, USA

<sup>§</sup>ZJU-UIUC Institute, Zhejiang University, Haining, China

Corresponding Author: Ruisheng Diao

\* means equal contribution; Email: ruishengdiao@intl.zju.edu.cn

**Abstract**—Long-term time series prediction has predominantly relied on Transformer and MLP models, while the potential of convolutional networks in this domain remains underexplored. To address this gap, we introduce a novel multi-scale time series reshape module, which effectively captures the relationships among multi-period patches and variable dependencies. Building upon this module, we propose MS-TVNet, a multi-scale 3D dynamic convolutional neural network. Through comprehensive evaluations on diverse datasets, MS-TVNet demonstrates superior performance compared to baseline models, achieving state-of-the-art (SOTA) results in long-term time series prediction. Our findings highlight the effectiveness of leveraging convolutional networks for capturing complex temporal patterns, suggesting a promising direction for future research in this field. The code is released on <https://github.com/Curyyfaust/TVNet>.

**Index Terms**—Long-Term Time Series Forecasting, CNN, Multi-Scale, Fourier transform

## I. INTRODUCTION

Long-term time series prediction is a crucial task with extremely wide applications in professional fields such as energy management [1] [2], weather forecasting [3], and health monitoring [4]. However, long-term time series forecasting tasks often involve complex multi-period scales and cross-variable dependencies [5], making the development of effective forecasting models a significant challenge. Real-world time series exhibit diverse variations across different temporal scales. To perform accurate time series forecasting, it is essential to adopt multi-scale modeling approaches that can capture features and dependencies from various time intervals. As illustrated in Figure 1, the same time series can be divided into smaller segments (in blue) or larger segments (in yellow), resulting in fine-grained or coarse-grained temporal features. In the figure, black arrows represent relationships between adjacent time steps, capturing local details, while colored arrows indicate relationships spanning longer time steps, reflecting global dependencies [6] [7] [8].

Currently, convolutional models have achieved notable progress in long-term time series forecasting. For instance, SCINet [10] discards causal convolutions and employs a recursive downsampling and convolutional interaction architecture to model complex temporal dynamics. Despite these advancements in capturing long-range dependencies, significant

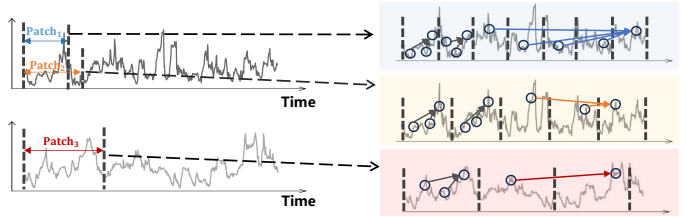


Fig. 1. Time series are divided into patches of varying sizes as temporal resolution [9]

challenges persist in long-term forecasting tasks. TimesNet [11] presents an innovative approach by transforming one-dimensional time series into two-dimensional representations and leveraging 2D convolution techniques from computer vision to enhance feature representation. ModernTCN [12] extends the application of convolution by utilizing large convolutional kernels to capture global temporal features. However, these models still fail to fully exploit the multi-scale characteristics of time series and the direct relationships across variables.

Multi-scale feature modeling has proven to be highly effective for correlation learning and feature extraction in fields such as computer vision and multimodal learning, but its potential has not been fully explored in time series forecasting. Existing methods like N-HiTS [13] model features at different resolutions through multi-resolution data sampling and hierarchical interpolation; Pyraformer [14] introduces a pyramid attention mechanism to extract features at various time resolutions; Scaleformer [15] proposes a multi-scale framework, but it increases model complexity due to the need to allocate predictive models at different time resolutions.

Through the aforementioned research, we have identified several issues in long-term time series forecasting at the current stage: (1) existing models lack adaptive multi-scale feature extraction; (2) there is a lack of a CNN-based network to extract patches and cross-variable dependencies within time series. To address these issues, this paper proposes MS-TVNet, an adaptive multi-scale 3D dynamic convolutional network for long-term time series forecasting. The innovations can be summarized as follows: (1) we proposed an adaptive Patch

module based on the Fourier transform to extract multi-scale features; (2) on this basis, a multi-scale dynamic convolution is proposed to extract patches and cross-variable dependencies. We have achieved results on public datasets that surpass the baseline state-of-the-art (SOTA) models.

The organization of the article is as follows: Section II provides a detailed description of the methods; Section III presents the experiments and results; Section IV concludes the article.

## II. METHOD

### A. Problem Statement

The goal of long-term time series prediction is to leverage a given historical sequence, denoted as  $\mathcal{X}_{\text{in}} = [\mathbf{x}_1, \dots, \mathbf{x}_L] \in \mathbb{R}^{L \times C}$ , to accurately forecast a subsequent sequence,  $\mathcal{X}_{\text{out}} = [\mathbf{x}_{L+1}, \dots, \mathbf{x}_{L+P}] \in \mathbb{R}^{P \times C}$ . Where,  $L$  represents the length of the historical time frame, which is the duration of the data we have observed and can use as a basis for predictions.  $P$  stands for the length of the predictive time frame, indicating how far into the future aim to forecast. Meanwhile,  $C$  signifies the dimensionality of the time series variables, meaning that each data point  $\mathbf{x}_i$  in the sequence is a vector with  $C$  features, capturing different aspects or features of the phenomenon being modeled.

### B. Framework

The proposed method is illustrated in Figure 2. The overall architecture of MS-TVNet is based on a Mixer-based framework and is composed of three key modules: *Multi-Patch*, *3D Dynamic Convolution*, and *Adaptive Aggregation*. Each of these modules plays a distinct role in enhancing Multi-Scale feature extraction and fusion. The *Multi-Patch* module is designed to capture local and global temporal dependencies across multiple time scales and the *3D Dynamic Convolution* module dynamically adjusts its receptive field to model complex multi-scale temporal interactions more effectively. Finally, the *Adaptive Aggregation* module integrates features from multiple paths to produce time series representations. In the following sections, we provide a detailed discussion of each component and its contribution to the model's overall performance.

*Multi-Patch Module:* This module utilizes the Fourier transform to extract multiple dominant periods embedded within the time series adaptively. By identifying these intrinsic periodic patterns, the time series can be segmented into patches that align with the discovered periods, enabling better structural representation and improved modeling efficiency. For a time series of length  $L$  with  $C$  features, the original format is represented as  $\mathcal{X}_{\text{in}} \in \mathbb{R}^{L \times C}$ , where each row corresponds to a specific timestamp and each column denotes a particular variable. To effectively capture temporal dependencies across varying scales, it is crucial first to identify the underlying periodic components. This is achieved by transforming the time series into the frequency domain using the Fast Fourier Transform (FFT), which enables the detection of frequency peaks corresponding to dominant periodicities. The resulting

spectral information serves as the foundation for adaptive patch segmentation, as detailed below:

$$\begin{aligned} \{f_1, \dots, f_k\} &= \arg \max_{f_* \in \{1, \dots, \lfloor \frac{T}{2} \rfloor\}} \text{Avg}(\text{Amp}(\text{FFT}(\mathcal{X}_{\text{in}}))) \\ p_i &= \left\lfloor \frac{T}{f_i} \right\rfloor, \quad i \in \{1, \dots, k\}. \end{aligned} \quad (1)$$

Where  $\text{FFT}(\cdot)$  and  $\text{Amp}(\cdot)$  represent the Fast Fourier Transform and the calculation of amplitude values, respectively. The amplitude of each frequency is computed by averaging across  $C$  dimensions using  $\text{Avg}(\cdot)$ . This corresponds to the patch length  $p_i = \frac{T}{f_i}$ , where  $f_i$  denotes the frequency.

*3D dynamic Convolution:* We first embed the input time series along the feature dimension, mapping it from  $C$  to a high-dimensional space of  $C_m$ , resulting in the embedded representation  $\mathcal{X}_{\text{in}} \in \mathbb{R}^{L \times C_m}$ . This step enhances the feature expressiveness. To segment the sequence into temporal patches ( $p_i$ ), we apply a one-dimensional convolutional layer (Conv1D) with a kernel size of  $P$ , effectively dividing  $\mathcal{X}_{\text{in}}$  into  $N = L/P$  patches. The output after convolution is denoted as  $\mathcal{X}_{\text{emb}} \in \mathbb{R}^{N \times P \times C_m}$ , where each patch preserves local temporal patterns over  $P$  time steps. Next, to further capture intra-patch structure, we split each patch into two equal-length sub-patches of size  $P/2$ , and then stack them along a new dimension, yielding the reshaped representation  $\mathcal{X}_{\text{emb}} \in \mathbb{R}^{N \times 2 \times (P/2) \times C_m}$ . This formulation enables the model to learn more nuanced dependencies within each patch. When using multiple patch lengths  $p_i$ , we can obtain a set of multi-scale embeddings  $\{\mathcal{X}_{\text{emb}}^1, \dots, \mathcal{X}_{\text{emb}}^k\}$ , enabling the model to capture dynamics at different temporal resolutions.

For each  $\mathcal{X}_{\text{emb}}^i$  we propose a dynamic convolutional method to capture the temporal dynamics within each patch. To clarify, the embedded representation  $\mathcal{X}_{\text{emb}}^i$  is envisioned as a collection of individual patches, denoted as  $(x_1, x_2, \dots, x_N)$ . The weight associated with the  $i$ -th patch, denoted as  $W_i$ , is hypothesized to be decomposable into the product of a constant *time base weight*  $W_b$ , which is common across all patches, and a *time varying weight*  $\alpha_i$ , which is unique to each patch.(see in Figure 3)

$$\tilde{x}_i = W_i \cdot x_i = (\alpha_i \cdot W_b) \cdot x_i, \quad (2)$$

To more accurately model the temporal dynamics of patches, the time-varying weight  $\alpha_i$  must account for all patches. We design an adaptive time-varying weight generation that considers the interaction between inter-patch and intra-patch, articulated as  $\alpha_i = \mathcal{G}(\mathcal{X}_{\text{emb}})$ . The function  $\mathcal{F}(\mathbf{v}_{\text{intra}})$  captures intra-patch features, initially applying 3D Adaptive Average Pooling to obtain  $\mathbf{v}_{\text{intra}}$ . For inter-patch channel modeling, a single-layer Conv1D is applied. The equations are as follows:

$$\alpha_i = \mathcal{G}(\mathcal{X}_{\text{emb}}) = 1 + \mathcal{F}(\mathbf{v}_{\text{intra}}) + \mathcal{F}(\mathbf{v}_{\text{inter}}) \quad (3a)$$

$$\mathbf{v}_{\text{intra}} = \text{AdaptiveAvgPool3d}(\mathcal{X}_{\text{emb}}) \quad (3b)$$

$$\mathcal{F}_{\text{intra}}(\mathbf{v}_{\text{intra}}) = \delta(\text{BN}(\text{Conv1D}^{C \rightarrow C}(\mathbf{v}_{\text{intra}}))) \quad (3c)$$

$$\mathbf{v}_{\text{inter}} = \text{AdaptiveAvgPool1d}(\mathbf{v}_{\text{intra}}) \quad (3d)$$

$$\mathcal{F}_{\text{inter}}(\mathbf{v}_{\text{inter}}) = \delta(\text{Conv1D}^{C \rightarrow C}(\mathbf{v}_{\text{inter}})) \quad (3e)$$

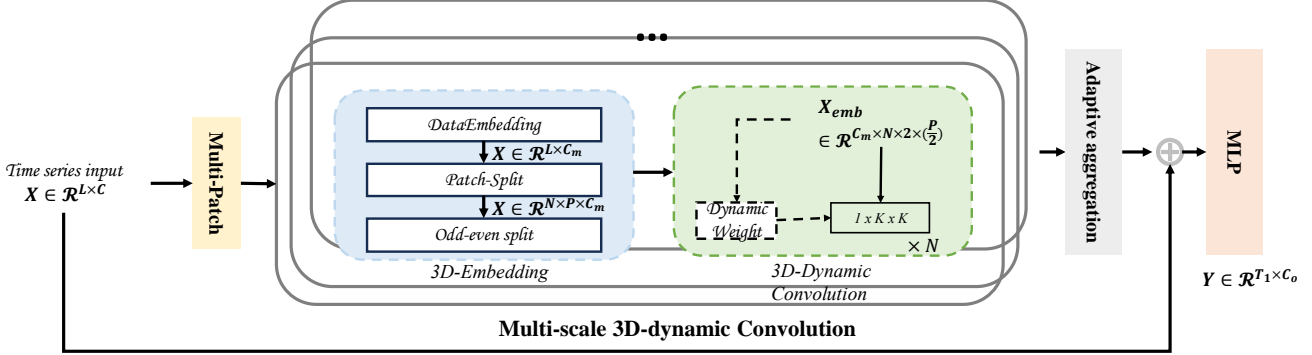


Fig. 2. The Framework of MS-TVNet

Here,  $\delta$  denotes the ReLU activation function.

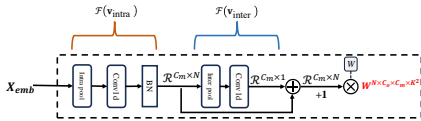


Fig. 3. The Time varying weight generation flow chart

After extracting features from each  $\mathcal{X}_{\text{emb}}^i$  using dynamic convolution, we obtain the 3D feature vector set  $\{\hat{\mathcal{X}}_{\text{emb}}^1, \dots, \hat{\mathcal{X}}_{\text{emb}}^k\}$ .

*Adaptive aggregation:* involves fusing  $k$  distinct 3D-feature vectors  $\{\hat{\mathcal{X}}_{\text{emb}}^1, \dots, \hat{\mathcal{X}}_{\text{emb}}^k\}$  for the subsequent layer. The amplitudes  $\mathcal{A}$  reflect the relative importance of selected frequencies and periods, corresponding to the importance of each transformed 3D tensor. We aggregate the 1D-representations based on these amplitudes:

$$\mathcal{A}_{f_1}, \dots, \mathcal{A}_{f_k} = \arg \text{Topk}(\text{Avg}(\text{Amp}(\text{FFT}(\mathcal{X}_{\text{in}})))) \quad (4a)$$

$$\hat{\mathcal{A}}_{f_1}, \dots, \hat{\mathcal{A}}_{f_k} = \text{Softmax}(\mathcal{A}_{f_1}, \dots, \mathcal{A}_{f_k}) \quad (4b)$$

$$\mathcal{X}_{\text{emb}} = \sum_{i=1}^k \hat{\mathcal{A}}_{f_i} \times \hat{\mathcal{X}}_{\text{emb}}^i \quad (4c)$$

The final prediction results are obtained using residual connections and an MLP, as shown in the following formulas:

$$Y = \text{MLP}(\mathcal{X}_{\text{emb}} + \mathcal{X}_{\text{in}}) \quad (5)$$

### III. EXPERIMENT AND RESULT

In this section, we evaluate the performance of MS-TVNet on public datasets using Mean Squared Error (MSE) and Mean Absolute Error (MAE) as our metrics. It is worth noting that, for these metrics, a lower value indicates a superior performance. To fully validate the effectiveness of the proposed method in this paper, we conducted comparisons on six public datasets (Exchange, ETTm2, ETTh1, Electricity, Weather, ILI) with nine baselines (TVNet [5], PatchTST [16], iTransformer [17], Crossformer [18], RLinear [19], MTS-Mixer [20], DLinear, TimesNet [11], and MICN [21]).

Our method and baselines are optimized using the Adam optimizer [22]. The learning rate starts at  $1e^{-4}$  and is halved when loss stagnates. The loss function used is MSE. We evaluate accuracy using  $MSE = \frac{1}{n} \sum_{i=1}^n (y - \hat{y})^2$  and  $MAE = \frac{1}{n} \sum_{i=1}^n |y - \hat{y}|$ . All models are run on a single NVIDIA 3090 GPU with 24 GB of memory.

The forecasting results are comprehensively presented in Table I. A clear trend is observed where the prediction accuracy tends to decline progressively as the forecast horizon length increases, reflecting the inherent challenges in long-term forecasting. In the comparative analysis of various forecasting models, MS-TVNet consistently outperforms its counterparts by achieving the MSE and MAE across multiple datasets and forecast horizons. This consistent performance underscores its robustness and ability to maintain high accuracy even in more complex forecasting scenarios. The visualization of these prediction results is further illustrated in Figure 4, which offers a clear graphical representation of the model's predictive capacity.

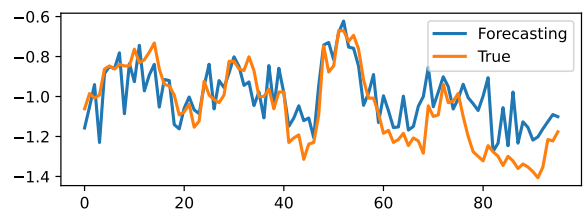


Fig. 4. The Forecasting result for ETTh1( $L=96$ )

*Computational Efficiency:* Figure 5 illustrates the efficiency and memory usage of different models. It can be seen from the figure that Transformer-based models have higher runtime (s/epoch) and memory usage compared to CNN-based models. Our proposed method does not employ the stacking approach used in TVNet, resulting in lower memory usage and runtime compared to TVNet. This indicates that the method proposed in this paper can achieve a balance between efficiency and utility.

*Input Length:* We evaluated the performance of our pro-

TABLE I

FORECASTING RESULT COMPARISON WITH DIFFERENT HORIZON LENGTHS. THE LOOKBACK LENGTH IS SET TO 24 FOR ILI AND 96 FOR THE OTHERS. **BOLD** INDICATES THE BEST RESULT, WHILE UNDERLINE INDICATES THE SECOND-BEST RESULT.

Models	MS-TVNet		TVNet		PatchTST		iTransformer		Crossformer		RLinear		MTS-Mixer		DLinear		TimesNet		MICN		
	MSE	MAE	MSE	MAE	MSE	MAE	MSE	MAE	MSE	MAE	MSE	MAE	MSE	MAE	MSE	MAE	MSE	MAE	MSE	MAE	
Exchange	96	0.087	0.217	<b>0.080</b>	<u>0.195</u>	0.093	0.214	0.086	0.206	0.186	0.346	0.083	0.301	0.083	0.200	0.081	0.203	0.107	0.234	0.102	0.235
	192	0.159	0.291	0.163	<b>0.285</b>	0.192	0.312	0.177	0.299	0.467	0.522	0.170	0.293	0.174	0.296	<b>0.157</b>	0.293	0.226	0.344	0.172	0.316
	336	0.284	<b>0.392</b>	0.291	<u>0.394</u>	0.350	0.432	0.331	0.417	0.783	0.721	0.309	0.401	0.336	0.417	0.305	0.414	0.367	0.448	<b>0.272</b>	0.407
	720	<b>0.642</b>	0.601	0.658	<b>0.594</b>	0.911	0.716	0.847	0.691	1.367	0.943	0.817	0.680	0.900	0.715	<u>0.643</u>	0.601	0.964	0.746	0.714	0.658
ETTm2	96	<b>0.137</b>	<b>0.250</b>	0.161	<u>0.254</u>	0.165	0.255	0.180	0.264	0.421	0.461	0.164	0.253	0.177	0.259	0.167	0.260	0.187	0.267	0.178	0.273
	192	<b>0.204</b>	<b>0.281</b>	0.220	0.293	0.220	0.292	0.250	0.309	0.503	0.519	0.219	0.290	0.241	0.303	0.224	0.303	0.249	0.309	0.245	0.316
	336	<b>0.264</b>	<b>0.318</b>	0.272	0.316	0.274	0.329	0.311	0.348	0.611	0.580	0.273	0.326	0.297	0.338	0.281	0.342	0.312	0.351	0.295	0.350
	720	<b>0.347</b>	<b>0.365</b>	0.349	<u>0.379</u>	0.362	0.385	0.412	0.407	0.996	0.750	0.366	0.385	0.396	0.398	0.397	0.421	0.497	0.403	0.389	0.406
ETTh1	96	<b>0.354</b>	<b>0.392</b>	0.371	0.408	0.370	0.399	0.386	0.405	0.386	0.429	0.366	0.391	0.372	0.395	0.375	0.399	0.384	0.402	0.396	0.427
	192	<b>0.390</b>	<b>0.404</b>	0.398	<u>0.409</u>	0.413	0.421	0.441	0.436	0.419	0.444	0.404	0.412	0.416	0.426	0.405	0.416	0.557	0.436	0.430	0.453
	336	<b>0.402</b>	<b>0.408</b>	<b>0.401</b>	0.409	0.422	0.436	0.487	0.458	0.440	0.461	0.420	0.423	0.455	0.449	0.439	0.443	0.491	0.469	0.433	0.458
	720	<b>0.437</b>	<b>0.446</b>	0.458	<u>0.459</u>	0.447	0.466	0.503	0.491	0.519	0.524	0.442	0.456	0.475	0.472	0.472	0.490	0.521	0.500	0.474	0.508
Electricity	96	0.139	<b>0.220</b>	0.142	0.223	<b>0.129</b>	<u>0.222</u>	0.148	0.240	0.187	0.283	0.140	0.235	0.141	0.243	0.153	0.237	0.168	0.272	0.159	0.267
	192	0.160	<b>0.238</b>	0.165	0.241	<b>0.147</b>	<u>0.240</u>	0.162	0.253	0.258	0.330	0.154	0.248	0.163	0.261	0.152	0.249	0.184	0.289	0.168	0.279
	336	0.159	0.260	0.164	0.269	0.163	<b>0.259</b>	0.178	0.269	0.323	0.369	0.171	0.264	0.176	0.277	0.169	0.267	0.198	0.308	0.161	0.259
	720	<b>0.176</b>	<b>0.273</b>	0.190	<u>0.284</u>	0.197	0.290	0.225	0.317	0.404	0.423	0.209	0.297	0.212	0.308	0.233	0.344	0.220	0.320	0.203	0.312
Weather	96	<b>0.140</b>	<b>0.198</b>	0.147	0.198	0.149	0.198	0.174	0.214	0.153	0.217	0.175	0.225	0.156	0.206	0.152	0.237	0.172	0.220	0.161	0.226
	192	<b>0.186</b>	<b>0.235</b>	0.194	<u>0.238</u>	0.194	0.241	0.221	0.254	0.197	0.269	0.218	0.260	0.199	0.248	0.220	0.282	0.219	0.261	0.220	0.283
	336	<b>0.230</b>	<b>0.269</b>	0.235	<u>0.277</u>	0.245	0.282	0.278	0.296	0.252	0.311	0.265	0.294	0.249	0.291	0.265	0.319	0.280	0.306	0.275	0.328
	720	<b>0.304</b>	<b>0.324</b>	0.308	<u>0.331</u>	0.314	0.334	0.358	0.347	0.318	0.363	0.329	0.339	0.336	0.343	0.323	0.362	0.365	0.359	0.311	0.356
IL1	24	<b>1.319</b>	<b>0.705</b>	1.324	0.712	1.319	0.754	2.207	1.032	3.040	1.186	4.337	1.507	1.472	0.798	2.215	1.081	2.317	0.934	2.684	1.112
	36	<b>1.182</b>	<b>0.765</b>	1.190	0.772	1.430	0.834	1.934	0.951	3.356	1.230	4.205	1.481	1.435	0.745	1.963	0.963	1.972	0.920	2.507	1.013
	48	<b>1.396</b>	<b>0.695</b>	1.456	0.782	1.553	0.815	2.127	1.004	3.441	1.223	4.257	1.484	1.474	0.822	2.130	1.024	2.238	0.940	2.423	1.012
	60	1.624	<b>0.782</b>	1.652	0.796	<b>1.470</b>	0.788	2.298	0.998	3.608	1.302	4.278	1.487	1.839	0.912	2.368	1.096	2.027	0.928	2.653	1.085

1<sup>st</sup> Count    37    5    4    0    0    0    0    1    0    1

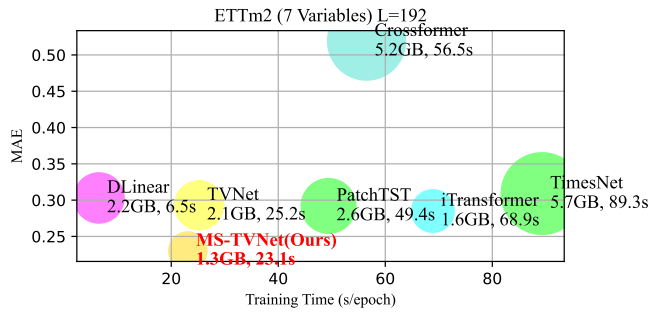


Fig. 5. Model efficiency comparison under the setting of L(prediction length) = 192 of ETTm2

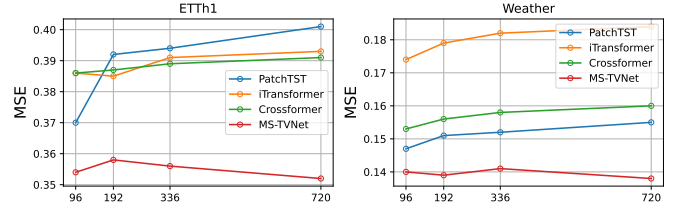


Fig. 6. The MSE results with different input lengths and same prediction lengths

posed method across a range of input lengths. As illustrated in Figure 6, the prediction performance of the Transformer-based model deteriorates as the input length increases. This may be attributed to the fact that the attention mechanism in Transformer-based models tends to capture periodic information incorrectly as the look-back window lengthens. In contrast, the method proposed in this paper fully accounts for periodicity. Therefore, as the look-back window expands, more periodic information can be captured, leading to a reduction in prediction error.

#### IV. CONCLUSION

In conclusion, MS-TVNet, our proposed multi-scale 3D dynamic convolutional neural network, has shown superior performance in long-term time series forecasting. With its innovative modules—such as Multi-Patch, 3D Dynamic Convolution, and Adaptive Aggregation—MS-TVNet effectively captures intricate temporal patterns and dependencies, offering high accuracy in predictions. Comprehensive evaluations across various datasets confirm its state-of-the-art performance, establishing its potential as a powerful tool for time series forecasting. These findings highlight the promising capabilities of convolutional networks in this domain, while suggesting potential avenues for future research, including architecture enhancements and domain-specific adaptations.

## REFERENCES

- [1] E. Nivolianiti, Y. L. Karnavas, and J.-F. Charpentier, “Energy management of shipboard microgrids integrating energy storage systems: A review,” *Renewable and Sustainable Energy Reviews*, vol. 189, p. 114012, 2024.
- [2] Z. Dong and T. Wang, “Artificial intelligence driving perception, cognition, decision-making and deduction in energy systems: State-of-the-art and potential directions,” *Energy Internet*, vol. 1, no. 1, pp. 27–33, 2024.
- [3] I. Price, A. Sanchez-Gonzalez, F. Alet, T. R. Andersson, A. El-Kadi, D. Masters, T. Ewalds, J. Stott, S. Mohamed, P. Battaglia *et al.*, “Probabilistic weather forecasting with machine learning,” *Nature*, vol. 637, no. 8044, pp. 84–90, 2025.
- [4] A. Yu, M. Zhu, C. Chen, Y. Li, H. Cui, S. Liu, and Q. Zhao, “Implantable flexible sensors for health monitoring,” *Advanced Healthcare Materials*, vol. 13, no. 2, p. 2302460, 2024.
- [5] C. Li, M. Li, and R. Diao, “Tvnnet: A novel time series analysis method based on dynamic convolution and 3d-variation,” *arXiv preprint arXiv:2503.07674*, 2025.
- [6] Z. Chen, M. Ma, T. Li, H. Wang, and C. Li, “Long sequence time-series forecasting with deep learning: A survey,” *Information Fusion*, vol. 97, p. 101819, 2023.
- [7] K. Yi, Q. Zhang, W. Fan, S. Wang, P. Wang, H. He, N. An, D. Lian, L. Cao, and Z. Niu, “Frequency-domain mlps are more effective learners in time series forecasting,” *Advances in Neural Information Processing Systems*, vol. 36, pp. 76656–76679, 2023.
- [8] W. Cai, Y. Liang, X. Liu, J. Feng, and Y. Wu, “Msgnet: Learning multi-scale inter-series correlations for multivariate time series forecasting,” in *Proceedings of the AAAI Conference on Artificial Intelligence*, vol. 38, no. 10, 2024, pp. 11141–11149.
- [9] P. Chen, Y. Zhang, Y. Cheng, Y. Shu, Y. Wang, Q. Wen, B. Yang, and C. Guo, “Pathformer: Multi-scale transformers with adaptive pathways for time series forecasting,” *arXiv preprint arXiv:2402.05956*, 2024.
- [10] M. Liu, A. Zeng, M. Chen, Z. Xu, Q. Lai, L. Ma, and Q. Xu, “Scinet: Time series modeling and forecasting with sample convolution and interaction,” *Advances in Neural Information Processing Systems*, vol. 35, pp. 5816–5828, 2022.
- [11] H. Wu, T. Hu, Y. Liu, H. Zhou, J. Wang, and M. Long, “Timesnet: Temporal 2d-variation modeling for general time series analysis,” *arXiv preprint arXiv:2210.02186*, 2022.
- [12] D. Luo and X. Wang, “Modernten: A modern pure convolution structure for general time series analysis,” in *The twelfth international conference on learning representations*, 2024, pp. 1–43.
- [13] C. Challu, K. G. Olivares, B. N. Oreshkin, F. G. Ramirez, M. M. Canseco, and A. Dubrawski, “Nhits: Neural hierarchical interpolation for time series forecasting,” in *Proceedings of the AAAI conference on artificial intelligence*, vol. 37, no. 6, 2023, pp. 6989–6997.
- [14] X. Huang, X. Lang, T. Guo, and L. Yu, “Improving pyraformer algorithm for forecasting of 500 kv transformer bushing data with three enhanced modules,” *Electric Power Systems Research*, vol. 241, p. 111360, 2025.
- [15] A. Shabani, A. Abdi, L. Meng, and T. Sylvain, “Scaleformer: Iterative multi-scale refining transformers for time series forecasting,” *arXiv preprint arXiv:2206.04038*, 2022.
- [16] H. Yi, S. Zhang, D. An, and Z. Liu, “Patchesnet: Patchst-based multi-scale network security situation prediction,” *Knowledge-Based Systems*, vol. 299, p. 112037, 2024.
- [17] Y. Liu, T. Hu, H. Zhang, H. Wu, S. Wang, L. Ma, and M. Long, “itransformer: Inverted transformers are effective for time series forecasting,” *arXiv preprint arXiv:2310.06625*, 2023.
- [18] Y. Zhang and J. Yan, “Crossformer: Transformer utilizing cross-dimension dependency for multivariate time series forecasting,” in *The eleventh international conference on learning representations*, 2023.
- [19] Z. Li, S. Qi, Y. Li, and Z. Xu, “Revisiting long-term time series forecasting: An investigation on linear mapping,” *arXiv preprint arXiv:2305.10721*, 2023.
- [20] Z. Li, Z. Rao, L. Pan, and Z. Xu, “Mts-mixers: Multivariate time series forecasting via factorized temporal and channel mixing,” *arXiv preprint arXiv:2302.04501*, 2023.
- [21] H. Wang, J. Peng, F. Huang, J. Wang, J. Chen, and Y. Xiao, “Micn: Multi-scale local and global context modeling for long-term series forecasting,” in *The eleventh international conference on learning representations*, 2023.
- [22] D. P. Kingma, “Adam: A method for stochastic optimization,” *arXiv preprint arXiv:1412.6980*, 2014.